EAI Endorsed Transactions
on Energy Web
Research Article EAI.EU

Energetic and exergetic study of a flat plate collector based solar water heater - investigation of the absorber size

Kumar Aditya Chandra[1], Bishal Podder[1], Supreme Das[1], Agnimitra Biswas[1*]

[1]Department of Mechanical Engineering, National Institute of Technology, Silchar, Assam, India-788010

Abstract

Small sized absorber in a flat plate solar collector is beneficial in terms of cost and minimum heat losses. However, its detailed thermal performance compared to standard size collector is still not fully understood. There is a paucity of research to appreciate thermal performance of solar water heating collector with consideration of a small absorber size (below 1m^2) and a standard absorber size (2 m^2). The present study attempts to investigate the energy and exergy efficiencies of flat plate solar water heating collector with two absorber plate areas (2 m^2 and 0.74 m^2) to enumerate size of the absorber required for improved first and second law thermal efficiencies of the collector. The efficiencies of these two collector designs are experimentally compared with the help of a test facility available in the site for given operating temperatures and rate of flow. The combined experimental uncertainty due to the measuring instruments and the measured parameters is also ascertained. The obtained results highlight the significance of the larger absorber size (2m^2) for higher thermal efficiency, and lower absorber size (0.74m^2) for higher exergetic efficiency. The highest thermal efficiency obtained is 77.38% for larger absorber size, and the highest exergy efficiency of 13.21% is obtained for lower absorber size collector. It is demonstrated that larger and lower absorber size of the collector have higher thermal efficiency and higher exergy efficiency, respectively, than some of the published works.

Keywords: Solar flat plate collector, absorber size, energy analysis, exergy analysis

Received on 02 June 2022, accepted on 17 February 2024, published on 20 February 2024

doi: 10.4108/ew.1350

1. Introduction

Solar energy has always been the best option for power generation among all renewable energy sources available today, and this is primarily due to its eco-friendly and bountiful nature. The solar irradiation incident on the earth's surface is nearly 1.5 x 10^{18} kWh/year, which is more than ten thousand times the worldwide energy consumption per year [1, 2]. The overall solar energy reportedly intercepted by the earth's surface is approximately 1363 W/m^2 [2]. Solar energy can be harvested in two ways: for producing Electricity (direct) and heat energy (indirect). Solar water heaters utilize solar energy indirectly to produce hot water for household and commercial applications. Its major components include a flat plate collector (FPC) for collection of solar energy, toughened glass, riser pipes and header pipe for carrying fluid, insulation and cover box. Solar FPC based water heaters are the oldest and most affordable form of water heating devices for residential and commercial establishments.

In the existing literature, various studies were reported pertaining to the enhancement in performance of solar FPCs like minimizing heat losses from the absorber surface with the help of selective coatings. Kafle et al. [3] observed that the performance of a FPC can be enhanced significantly by incorporating black nickel as a selective coating. In another study, Zamora et al. [4] employed black cobalt as a selective coating and obtained a solar absorptance of 95%. Liu et al. [5] documented a comprehensive review on selective coatings based on different types of nanomaterials and obtained their optical and thermal properties for high temperature applications. An experimental study was presented by Reddy et al. [6] using sand as an absorber

*Corresponding author. Email: agnibis@yahoo.co.in

coating material for solar air collector and obtained a significant enhancement in its performance.

Heat transfer from the surface can also be enhanced by using various designs of extended surface [7]. Kabeel et al. [8] studied the performance of a FPC with extended fins for varying mass flow rates and fin heights. The highest thermal efficiency achieved was 57% for mass flow rate and fin height of 0.04 kg/s and 8 cm, respectively.

Kumar and Chand [9] studied the thermal performance of a solar air heater with fins combined with twisted tape for a wide range of flow rates, turn ratios and solar radiation. The results revealed that the thermal efficiency increases by a maximum of 22.56% with the twisted inserts at 0.025kg/s rate of flow. Saravanan and Jaisankar [10] experimentally investigated and compared the performance of a square cut and a V cut helix twisted tape for various design configurations. It was reported that by inserting V cut tape, the thermal performance of the collector increased significantly. In another study, Vengadesan and Senthil [11] studied the performance of a water based FPC with rectangular inserts for a range of mass flow rates, and a maximum instantaneous thermal efficiency of 72.93% was achieved at a mass flow rate of 0.025kg/s.

A few works related to wavy and corrugated absorber surfaces has also been investigated by several researchers in order to improve the overall performance of air collector. Reddy et al. [12] demonstrated an outdoor study of solar air collector with corrugated design of an absorber surface, by varying tilt angles and mass flow rates. Tuncer et al. [13] evaluated the performance of a solar air heater with v-groove absorber design and investigated for various multi pass systems. Kabeel et al. [14] introduced a number of baffle plates in a solar air collector, and also attached several guide blades at the entry region of the collector. A maximum daily efficiency of 83.8% was obtained at 0.04kg/s of flow rate. An experimental analysis of a plain and a corrugated type of solar air collector was performed by Debnath et al. [15] for a wide range of mass flow rates and inclination angle. It was observed that the efficiency of the corrugated design was increased by 9% as compared to the plain absorber sheet. A similar type of comparative study between flat and wavy absorber sheet for a photovoltaic- thermal air collector was performed by Jha et al. [16]. It was revealed that the wavy absorber sheet attained higher thermal efficiency than the plain sheet, while operating under similar set of inlet conditions. Jouybari et al. [17] demonstrated an innovative approach to augment the thermal performance of a FPC by incorporating a metallic porous medium along with silica nanofluid inside the channel. It was found that the thermal efficiency rose up to 8% with 0.6% volume fraction of the nanofluid. Hussein and Farhan [18] experimentally investigated an air-based collector with fins made of metallic foams, fixed underneath an absorber sheet with varying design configurations. They observed that the maximum thermal efficiency of the FPC was 86%, at 0.05 m^3/s of discharge. Das et al. [19] performed an experimental investigation using sand as an absorber coating under different solar radiations and mass flow rates.

It is evident that absorber plates of different sizes will have differential heating effects and heat losses. The aperture area of the absorber surface is responsible in determining the quantity of solar radiation received by the FPC. As such, it is essential that its size is judiciously selected for maximum absorption of heat with minimal heat losses from the upper glazing surface. In this direction, a small area of the aperture plane can concentrate more radiant energy density with reduced top heat loss compared to large aperture plane. However, the effect of the absorber size needs to be evaluated in regard to the energetic and exergetic performances of the collector. Previous works have estimated these performances for different absorber sizes in order to develop improved FPC designs. Farhan et al. [20] performed energy and exergy analysis of a V-shape absorber combined with twisted coil for solar air heater performance for different design dimensions of corrugation and tape insert and Reynolds number. The aperture plane area was kept fixed at 1.5 m^2 and their design exhibited improved thermal efficiency up to 76.7% compared to only corrugated solar air heater. Kumar et al. [21] compared the enhancement in exergetic performance of a solar FPC of aperture area 1.8 m^2 with a rod and a tube arrangement. They concluded that the rod insert mechanism provided higher exergetic efficiency than the tube and the normal riser tube based FPC. The maximum exergy efficiencies reported were 11.3%, 10.9% and 8.3% for the rod heat transfer enhancer, tube heat transfer enhancer and the normal riser tube based FPC, respectively. Jafarkazemi and Ahmadifard [22] investigated the variations of energetic and exergetic efficiencies of a FPC for an absorber aperture area of 1.59 m^2 for different water flow rates and water inlet temperatures. They concluded that the overall performance of the FPC could be enhanced by designing the system for lower mass flow rates with water temperature 40°C higher than the ambient. The maximum energetic and exergetic efficiencies obtained were around 73% and 7.5%, respectively. Gunjo et al. [23] experimentally studied the effect of various operating parameters of a FPC having absorber area 1.65 m^2. It was shown that thermal efficiency is directly proportional to ambient temperature, solar irradiance, and water flow rate, whereas it is inversely proportional to water inlet temperature, while the maximum value was obtained as 58%.

Some more recent works entailed the investigation of nanofluid as heat absorbing medium to improve the thermal performance of FPC. Experimental test runs were performed for different mass flow rates of three different types of nanofluids from 0.8 to 1.6 kg/min for a FPC with absorber area 0.46 m^2 [24]. It was observed that the thermal efficiency and exergy efficiency improved with the rise in mass flow rates. In addition, it was observed that the graphene based nanofluids achieved the highest efficiency of 17.45% at a water rate of 1.6 kg/min.

Farhat et al. [25] performed an exergetic optimization of a FPC by varying the absorber aperture area between 1 and 10 m^2 and mass flow rates between 0.001 and 0.009 kg/s. It was concluded that the exergy efficiency increased by increasing the incident solar irradiance on the absorber plate. An increase in fluid inlet temperature also led to an increase in exergy efficiency up to a certain limit, beyond which the

exergy efficiency decreased. Luminosu and Fara [26] also performed a similar study for demonstrating the effect of exergy on flow rate and absorber surface area. The exergy analysis was performed by considering the similarity between inlet temperature and the ambient. The absorber aperture area was varied between 1 m^2 and 10 m^2, while the water rate was varied between 0.001 and 0.015 kg/s.

Tong et al. [27] performed a comparative analysis of a solar FPC using water and two different nanofluids for absorber area of 1.87 m^2 and water rate of 0.047 kg/s and reported higher energetic and exergetic efficiency (78% and 3.2%, respectively) for the nanofluid (Al_2O_3) compared to water. Rostami et al. [28] used water-nanofluid in an elliptical heat pipe based solar FPC (aperture area 1.593 m^2) for its exergetic performance optimization and demonstrated improved energetic and exergetic efficiency of their novel heat pipe FPC with water nanofluid. The maximum exergetic efficiency obtained by them was 7.1%. Gunjo et al. [29] used a twisted riser tube with an absorber plate aperture area of 1.65 m^2 and obtained the highest energetic and exergetic efficiencies of 71% and 6.3% (for solar insolation 1000 W/m^2), respectively.

Numerous experimental and computational works have been reported in literature pertaining to the improvement in thermal performance of FPC based solar air heaters; but in the similar line, works related to FPC based solar water heaters are relatively few. Also, very few research studies have delved into the analysis of thermal performance of FPCs considering standard absorber size i.e. 2m^2 and absorber sizes less than 1m^2. Although the studies conducted by Farhat et al. [25] and Luminosua & Fara [26] are in the same direction of the present work, the absorber sizes were considerably larger than the present work. Also, the mass flow rates for which the studies were conducted were of the order of 10^{-3} kg/s, which is much lower than the present work.

This paper attempts to enhance the thermal performance of FPC based water heaters by comparing the influence of absorber surface area on energetic and exergetic efficiency and considering higher values of mass flow rates following a standard code (IS 12933). Two absorber plates having surface areas of 2m^2 and 0.74m^2 are considered and their performances are compared for a fixed value of inlet and ambient temperature using the experimental facilities available at the site.

2. Mathematical Modelling

Here a detail mathematical modeling is presented.

2.1. Heat gain rate from the collector

The heat gain (q_u) can be obtained by Hottel-Whiller Bliss equation and is expressed as follows:

$$q_u = F_r A_p [S - U_l(T_i - T_a)] \quad (1)$$

Where, T_i = fluid inlet temperature and is usually a known quantity,
F_r =heat removal factor,
A_p = absorber surface area,
S = absorbed solar radiant energy by the collector,
U_l = overall heat loss coefficient,
T_a = ambient temperature.

2.2. Outlet temperature of water

The outlet temperature of the water can be evaluated from the heat balance equation and is given by [31]:

$$q_u = mC_P(T_{out} - T_{in}) \quad (2)$$

Where, T_{out} = outlet water temperature,
T_{in} = inlet water temperature to the collector,
$\dot{m}$ = mass flow rate,
C_p = specific heat of water.

2.3. Thermal efficiency of the FPC (η_i)

The instantaneous thermal efficiency of the FPC is expressed as [32]:

$$\eta_i = \frac{q_u}{A_p I_t} \quad (3)$$

Where, I_t is the solar irradiance on the tilted flat plate collector.

2.4. Exergetic Efficiency

Exergetic Efficiency is an efficiency parameter, and it is the ratio of the increase of the exergy due to water flow to the exergy of solar irradiation on the solar collector. Exergetic efficiency of a FPC can be expressed as:

$$\eta_{ex} = \frac{mC_p(T_{out} - T_{in} - T_a \ln\frac{T_{out}}{T_{in}})}{I_t A_p (1 - \frac{T_a}{T_s})} \quad (4)$$

Where, T_s is the sun temperature and considered as 4500K in this study [30].

2.5. Estimation of experimental uncertainty

Any experimental work is considered incomplete without uncertainty i.e., relative error analysis; hence due attention has been given to the same in this work. Uncertainties in experimental work may be categorised into Type A and Type B. Type A uncertainty relates to the uncertainty during the performance of the experiments and Type B relates to the uncertainty or traceability of the measuring instruments obtained during calibration. Many earlier research studies have implemented Type A uncertainty or simply relative error in their experimental works. In this work however, the combined uncertainty has been implemented by combining the uncertainties in measurement process and in the calibration of the measuring instruments.

Calculation of Type A uncertainty:

Let us consider 'n' number of variables: I_1, I_2, I_3……. I_n, which can be considered as measured parameters of the

present work. The mean value of these variables can be calculated as:

$$\bar{X} = \frac{1}{n}\sum_{i=1}^{n} I_i \quad (5)$$

Deviation of the values of measured variables from the mean value may ascertain as follows:

$$d_1 = (I_1 - \bar{X})^2, d_2 = (I_2 - \bar{X})^2, ...dn = (In - \bar{X})^2 \quad (6)$$

$$\sum d^2 = \sum_{i=1}^{n} (I_i - \bar{X})^2 \quad (7)$$

Therefore, experimental standard deviation may be expressed as:

$$\sigma = \sqrt{\frac{\sum d^2}{n}} \quad (8)$$

Hence Type A uncertainty is given by:

$$u_A = \frac{\sigma}{\sqrt{n}} \quad (9)$$

Calculation of Type B uncertainty:

The standard deviation is given by-

$$\sigma_1 = \frac{a_1}{k} \quad (10)$$

Where a_1 is expanded uncertainty of the calibration results of the measuring instruments and k = 1.96 for 95% confidence level considered in this work.

Hence Type B uncertainty can be given by-

$$u_B = \sqrt{\sigma_1^2} \quad (11)$$

The combined uncertainty of the experimental study can therefore be estimated as:

$$u_C = \sqrt{(u_A)^2 + (u_B)^2} \quad (12)$$

In this work, the combined experimental uncertainty for all measured parameters (i.e. temperature, radiation and mass flow rate) was estimated as ± 0.13, i.e. 13%.

3. Experimental Setup and Procedure

The assumptions are presented first, and then the experimental setup and experimental procedure are discussed.

3.1. Assumptions

The performance analysis of the solar FPC has been investigated on the basis of a few assumptions as described below:

1. Area of the header pipes is assumed to be negligible.
2. No absorption of solar energy by the glass covers.
3. Uniform flow through the header pipes.
4. Uni-dimensional steady heat flow from the glass and absorber plate.
5. Temperature difference across the glass is insignificant.
6. Glass is transparent to infrared radiation.
7. Temperature gradient in the tubes is negligible.
8. There is a steady-state flow through the collector.

3.2. Experimental Setup

Figure1 represents the experimental setup of the FPC inclined at 40° and having a collector aperture area of 2 m^2. Similarly, the other collector of 0.74m^2 collector aperture area was also inclined at 40°. The recommended value for tilt angle of any solar device for operating in winter season is around: 'latitude+15°', whereas for summer season the recommended value for the same is around: 'latitude-15°' [2]. In the present case, the latitude is 23.45°, and the experimental study was performed during winter season, therefore, the inclination angle of 40° was chosen in this case. The solar noon of the place is 11:30 hours. The specifications of both the collectors are presented in Table 1.

Table 1. Specification of the collectors

Collector Parameters	Collector1 (A_p = 2m^2)	Collector 2 (A_p = 0.74m^2)	Material
Thickness of the absorber plate (δ_p)	0.007m	0.00012m	Al
Outer diameter of the riser tubes (D_o)	0.0137m	0.0127m	Cu
Inner diameter of the riser tubes (D_i)	0.0127m	0.0117m	Cu
Centre to centre distance between the riser tubes (w)	0.105m	0.115 m	--
Emissivity of the glass cover (ϵ)	0.88	0.88	Toughened glass with single glazing
Emissivity of the absorber plate (ϵ_p)	0.15	0.12	Al
Coefficient of thermal expansion of glass	0.19	0.19	--
Thermal conductivity of the plate	210 W/mK	210 W/mK	--
Thermal conductivity of the insulation	0.04 W/mK	0.04 W/mK	Glass wool

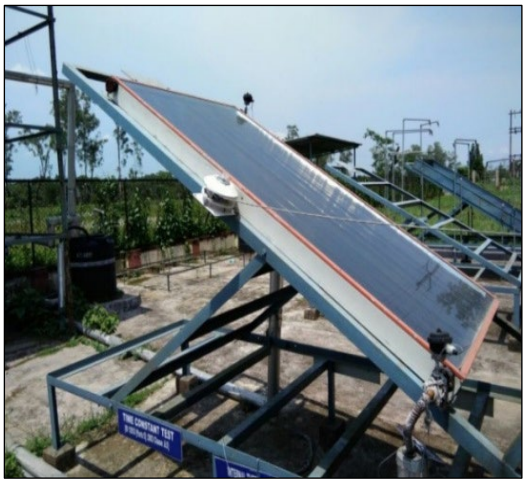

(a)

(b)

Figure 1. (a) FPC with 2 m^2 absorber area inclined at 40° (b) Tank for supplying hot water at RTC, NIT Silchar

3.3. Experimental procedure

Experiments were performed on the setup at an interval of 15 minutes from 10.00 am to 2.00 pm on a clear sky day. A constant mass flow rate of 2.7 lpm (i.e. 0.045 kg/s) was maintained at the inlet to the collector (according to the IS 12933 code) with the help of an electromagnetic flowmeter (least count 0.1 lpm) as shown in fig 1(a). Thus, considering the aperture area of the given absorbers, the water rates were 0.0225 kg/s-m^2 and 0.0608 kg/s-m^2 through the absorber aperture area 2 m^2 and 0.74 m^2, respectively. During experimentations, the inlet temperature was constantly maintained at 30°C and 40°C. This was done with the help of a heating coil, placed inside the constant pressure head tank, as shown in fig.1 (b). These inlet temperatures were similar to the ambient conditions at the testing site. A temperature control mechanism (PID controller) was incorporated to fix the heating coil temperature to the desired level. A mechanical stirrer was placed inside the tank, which was also controlled by the PID controller. A rubber hose pipe was used for connecting the constant pressure head tank to the inlet of the collector through an electromagnetic flowmeter. The connection was properly insulated by aluminium casing with interior glass wool packing for minimum heat loss. The heated water rose up to the top of the collector, i.e. the outlet due to natural convection. Another insulated rubber hose pipe was used to circulate the hot water from the outlet point to a storage tank. In the tank, the hot water from the collector was mixed with cold water already present in the tank, thus reducing its temperature. This water is then lifted by a circulating pump and delivered to the constant pressure head tank. As a result, a closed loop system was preserved. Temperature sensors were installed at the collector's inlet and outlet points, as shown in Fig.1 (a). Solar radiation data (global solar radiation) was collected on an hourly basis during the experiments utilising a solar pyranometer from the Regional Testing Center (RTC) laboratory in the venue. The pyranometer was positioned parallel to the collector's top plane, as shown in Fig.1 (a). The water outlet temperature was recorded at regular intervals, and the instantaneous thermal efficiencies were calculated using the formula described earlier. The tests were carried out under the identical operating conditions on the two distinct collector designs, as specified in Table 1.

4. Results and Discussion

The thermal performance of a FPC with varied absorber surface areas (i.e. 2 m^2 and 0.74 m^2) was evaluated on the basis of both energy and exergy efficiency. During the experimentation, 0.045 kg/s of water rate was maintained and inlet temperatures of 30°C and 40°C were chosen. The temperatures of the collector inlet were chosen depending on the climate of tropical regions such as India. The mass flow rate was chosen using the IS 12933 standard code. The temperature difference, usable energy gains by the collector (in kJ/hr), thermal efficiency, and exergetic efficiency of the collector were all examined. This section presents and discusses the various findings.

Figures 2(a) and (b) show the temperature difference between the collector's outlet and inlet as a function of time for absorber aperture areas of 2 m^2 and 0.74 m^2 respectively, under various daily average solar irradiations and constant ambient temperature 30°C. These graphs illustrate that as time passes, the temperature difference increases until around 11.30 hrs. After that, the temperature difference decreases for all values of solar radiation. This decrease in temperature difference is a result of lower radiation levels during afternoon period. The same phenomenon could be observed for both the collectors with the highest temperature difference being recorded for a solar radiation of 740 W/m^2. Maximum temperature difference of 7.28°C was obtained for the larger collector (2 m^2) whereas the same was obtained as 1.10°C for the smaller collector (0.74 m^2).

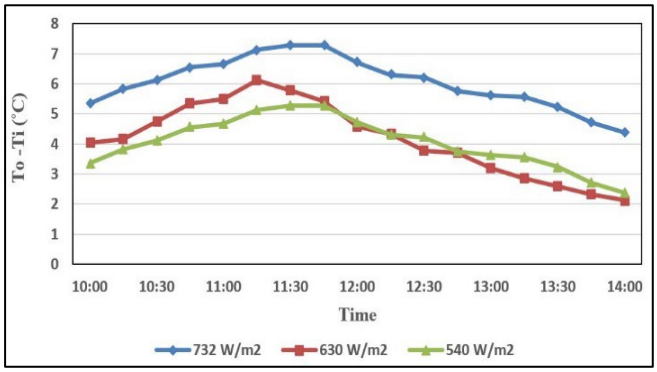

Figure 2(a). Variation of outlet and inlet temperature difference with time at different daily average irradiation for 2 m^2 absorber area and ambient temperature 30°C

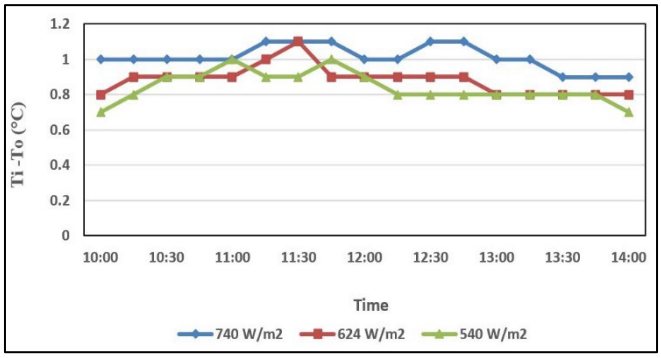

Figure 2(b). Variation of outlet and inlet temperature difference with time at different daily average irradiation for 0.74 m^2 absorber area for ambient temperature 30°C

Figures 3(a) and (b) demonstrate the variation in useful energy absorbed by the collector as a function of time at varied solar radiation levels and constant ambient temperature 30ºC for absorber aperture areas of 2 m^2 and 0.74 m^2, respectively. Due to the higher temperature difference at the solar radiation of 740 W/m^2, useful energy is higher regardless of the absorber surface area. Also, it is observed that the larger collector absorbs more useful energy due to the transference of higher radiation flux through the glazing. At solar radiation of 740 W/m^2, the 2m^2 absorber recorded a maximum useful energy gain of 1369.37 kJ/hr, whereas the 0.74m^2 absorber recorded just 230.34 kJ/hr.

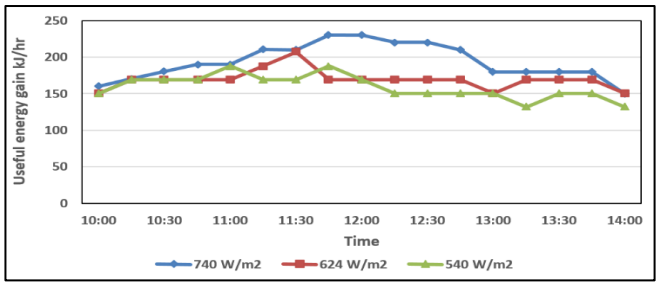

Figure 3(a). Variation of useful energy gain with time at different daily average irradiation for 2 m^2 absorber area for ambient temperature 30°C

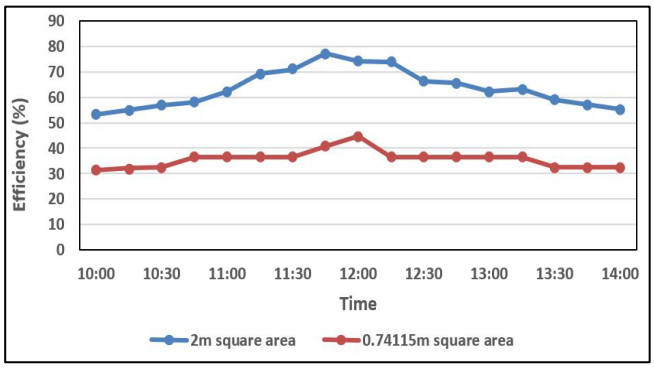

Figure 3(b). Variation of useful energy gain with time at different daily average irradiation for 0.74 m^2 absorber area for ambient temperature 30°C

Table 2 shows the results obtained from the comparison of collector performance for two different absorber areas, i.e. 2 m^2 and 0.74 m^2 for inlet temperatures of 30ºC. Further, Table 2 also shows comparable findings when the input temperature is set to 40°C. It is observed that regardless of the absorber size, both the temperature difference and the absorbed usable energy by the collectors are lower at this temperature than at 30ºC. This can be attributed to an increase in convective and re-radiation losses from the plate surface as a result of the increased ambient temperature.

Figure 4 depicts the comparison of the two collectors' instantaneous thermal efficiency for a typical solar day with an ambient temperature of 30°C. It is evident that the efficiencies are substantially higher for the collector with a 2 m^2 absorber aperture area, which can be attributed to the larger collector absorbing a greater amount of useful energy. Maximum efficiency of 77.38% was obtained for the 2 m^2 collector as compared to 44.74% for the collector having an absorber area of 0.74 m^2. However, at 40°C ambient temperature, the former collector's maximum efficiency declines to 57.52% and the latter collectors to 40.67%, as shown in table 2. The loss in efficiency at this higher temperature is due to the drop in absorbed useful energy at 40°C.

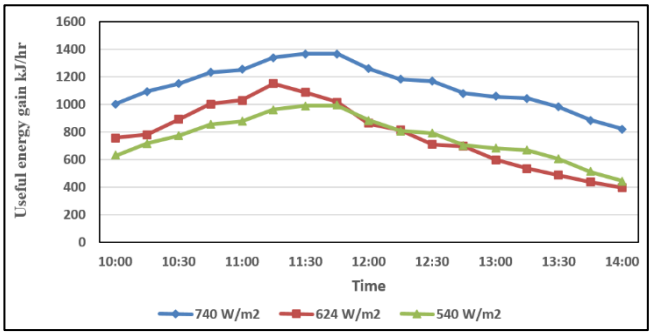

Figure 4. Comparison of instantaneous thermal efficiencies of the two absorber designs for a solar day for ambient temperature 30°C

Figures 5(a) and (b) demonstrate the variations in exergetic efficiency of the two collectors with respect to time at different solar radiations and inlet temperature 30ºC. The exergetic efficiency drops as solar radiation increases, which is due to a decline in the collector's work potential at higher radiation levels. Because exergetic efficiency is inversely proportional to solar radiation, as shown earlier in equation 4, higher exergetic efficiency is attained at a lower solar radiation of 540 W/m^2. Furthermore, the exergetic efficiency of the larger collector (2 m^2 absorber size) initially decreases till noon due to a rise in temperature difference. The same gradually increases as the temperature difference diminishes during the afternoon period. However, in the smaller collector (0.74 m^2 absorber size), the exergetic efficiency constantly increases with time from the beginning due to fewer losses from the collector's top owing to a smaller temperature drop. A comparison between the exergetic efficiencies of the two collector designs also show that the exergetic losses associated with the smaller absorber aperture area (i.e. 0.74 m^2) are much less, thus leading to higher exergy efficiencies. Whilst the maximum exergy efficiency of 9.99% was recorded for the smaller collector, the same was recorded as 5.08% for the larger collector with absorber aperture area of 2 m^2. These exergetic efficiencies further increase to 13.21% and 6.44% respectively, when the inlet water temperature is raised to 40ºC. This is due to the fall in temperature difference (outlet – inlet) in both the collectors.

Finally, Table 3 compares the results of the current absorber designs to some of the designs in the literature with water as the coolant. It demonstrates that the current absorber design with a 2 m^2 size has enhanced thermal performance in terms of thermal efficiency, both maximum and instantaneous. For e.g., compared to literature [27], the present maximum thermal efficiency is higher by 21.6% for absorber side 2 m^2. It can also be seen that the absorber size 0.74 m^2 has higher exergetic efficiency in comparison to the designs mentioned in previous literature. For e.g., compared to literature [22], the present maximum exergy efficiency is higher by 33.2% for absorber side 0.74 m^2 Furthermore, the rate of flow in the order of 10^{-2} is beneficial for the collector's overall thermal performance, as shown in table 3, based on the results of the present study and previous literature.

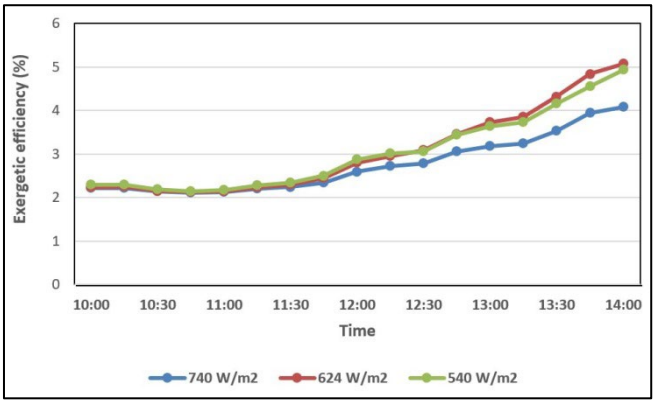

Figure 5(a). Variation of Exergetic efficiency with time at different daily average irradiation for 2 m^2 absorber area for ambient temperature 30°C

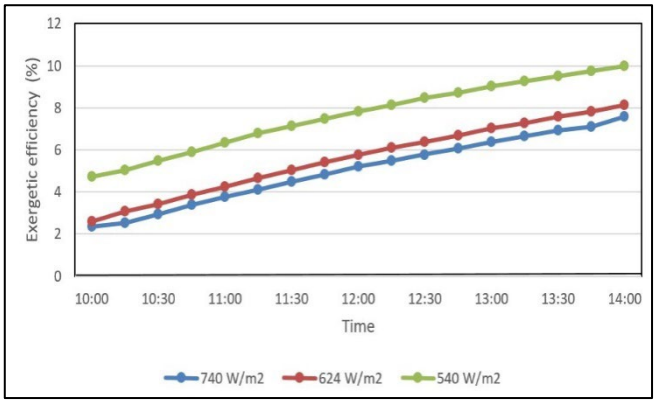

Figure 5(b). Effect of Exergetic efficiency at daily average irradiation for 0.74 m^2 absorber area for ambient temperature 30°C

Table 2. Results of comparison of collector performance for two different absorber areas

Ambient temp(ºC)	Mass flow rate (lpm)	Maximum fluid temperature difference (ºC)		Maximum useful energy gain (kJ/hr)		Maximum thermal efficiency (%)		Maximum exergetic efficiency (%)	
		A_p = 2 m^2	A_p = 0.74 m^2	A_p = 2 m^2	A_p = 0.74 m^2	A_p = 2 m^2	A_p = 0.74 m^2	A_p = 2 m^2	A_p = 0.74 m^2
30	2.7	7.28	1.1	1369	230	77.38	44.74	5.08	9.99
40	2.7	5.12	0.9	982	207	57.52	40.67	6.44	13.1

Table 3. Comparison of present results with some of the published works with water as the working fluid

Parameter	Jafarkazemi & Ahmadifard [22]	Farahat et al. [25]	Luminosua & Fara [26]	Sakhrieh & Al-Ghandoor [30]	Tong et al. [27]	Present study
Absorber area (m^2)	1.59	9.14	3.3	1.65	1.87	2 & 0.74
Mass flow rate (kg/s)	$1x\ 10^{-2}$	$8.7\ x\ 10^{-3}$	$0.34x\ 10^{-4}$	$3.3\ x\ 10^{-2}$	$4.7\ x\ 10^{-2}$	$4.5\ x\ 10^{-2}$
Max. thermal efficiency	75%	46.81%	43%	80.1%	63.6%	77.38% & 44.74%
Max. exergetic efficiency	7.5%	3.89%	3.6%	--	--	5.08% & 9.99%
Instantaneous efficiency (10 a.m)	--	39.6%	38%	49.7%	--	53.26% & 31.26%
Instantaneous efficiency (12 noon)	--	39.09%	39%	60.8%	--	74.36% & 44.74%
Instantaneous efficiency (2 p.m.)	--	41.97%	43%	80.1%	--	55.36% & 32.53%
Instantaneous exergetic efficiency (10 a.m)	--	1.65%	1.6%	--	--	2.29% & 4.74%
Instantaneous exergetic efficiency (12 noon)	--	2.55%	2.5%	--	--	2.87% & 7.83%
Instantaneous exergetic efficiency (2 p.m.)	--	2.95%	2.9%	--	--	5.08% & 9.99%

5. Conclusions

The present study demonstrates the thermal performances of solar FPC based water heaters with two different absorber plate aperture areas (2 m^2 and 0.74 m^2) are experimentally compared for two different ambient temperatures (30°C and 40°C) and three different values of solar irradiation, viz. 540 W/m^2, 624 W/m^2 and 740 W/m^2, and a fixed operating mass flow rate of 2.7 lpm (i.e. 0.045 kg/s) using laboratory facilities available at the venue. The combined uncertainty has been ascertained by combining the uncertainties in measurement process and in the calibration of the measuring instruments. The following findings have been derived from the study:

- Regardless of solar radiation, the difference between inlet and outlet temperatures of the 2 m^2 absorber is greater than that of the 0.74 m^2 absorber. At 740 W/m^2, the highest temperature difference was recorded at 7.28°C for the former collector and 1.10°C for the latter collector.
- The thermal gain of the flat plate collector is directly proportional to the absorber aperture area. The maximum useful energy gain for the 2 m^2 absorber was recorded at 1369.37 kJ/hr compared to 230.34 kJ/hr for the 0.74 m^2 absorber area at 740 W/m^2.
- The exergetic efficiency of the 2 m^2 absorber is lower than that of the 0.74 m^2 absorber, owing to more exergy destruction in the larger system due to a higher temperature difference. The former collector's

maximum exergetic efficiency was recorded at 6.44% as compared to 13.21% in the latter one.

- In terms of thermal efficiency, a $2m^2$ absorber is more efficient as compared to a 0.74 m^2 absorber. The 2 m^2 absorber size has a maximum thermal efficiency of 77.38%, whereas the latter has the maximum thermal efficiency of 44.74%.
- The significance of the larger absorber size (2 m^2) for higher thermal efficiency and the smaller absorber size (0.74 m^2) for higher exergetic performance of the FPC for rate of flow of the order of 10^{-2} is highlighted by comparisons of thermal performances of the present absorber designs with published works.

In the present study the meteorological condition of the geographical location (Latitude- 24.8ºN, 92.7ºE) was taken into consideration. As the studied region falls under hot and humid region conditions, therefore, the system is applicable for all the locations having a sub-tropical climate. Moreover, as the meteorological cycle repeats every year, therefore, the study can provide a better understanding of the collector performance in any sky condition. In the future study, a solar simulator can be used for varying the solar radiation manually and the overall performance can be evaluated for any solar radiation. Further in this study only comparison of absorber sizes was done; therefore, as a future scope, the optimization of the absorber size for sub-tropical climatic conditions can also be carried out.

Acknowledgements

The authors acknowledge with thanks the technical support provided by the Regional Test Centre of Mechanical Department of National Institute of Technology Silchar, Assam, India.

References

[1] Dutta D., Podder B., Biswas A. Solar Energy Potential of Silchar, Assam, India-A Resource Assessment. Advances in Optical Science and Engineering, Springer Proceedings in Physics. 2015; Vol. 166:119.

[2] Duffie, J.A., Beckman, W.A. and Blair, N. Solar engineering of thermal processes, photovoltaics and wind. John Wiley & Sons.2020.

[3] Kafle, B.P., Basnet, B., Timalsina, B., Deo, A., Malla, T.N., Acharya, N. and Adhikari, A. Optical, structural and thermal performances of black nickel selective coatings for solar thermal collectors. Solar Energy.2022; Vol.234:262-274.

[4] Herrera-Zamora, D.M., Lizama-Tzec, F.I., Santos-González, I., Rodríguez-Carvajal, R.A., García-Valladares, O., Arés-Muzio, O. and Oskam, G. Electrodeposited black cobalt selective coatings for application in solar thermal collectors: Fabrication, characterization, and stability. Solar Energy. 2022; Vol. 207:1132-1145.

[5] Liu, B., Wang, C., Bazri, S., Badruddin, I.A., Orooji, Y., Saeidi, S., Wongwises, S. and Mahian, O. Optical properties and thermal stability evaluation of solar absorbers enhanced by nanostructured selective coating films. Powder Technology.2021; Vol.377:939-957.

[6] Reddy, J., Roy, S. and Das, B. Performance evaluation of sand coated absorber based solar air collector. Journal of Building Engineering.2021; Vol.44:102973.

[7] Babu J.S., Senthilvel S., Gregory F.P, Gopi T. Springer Proceedings in Energy, Adv. Energy Res. Vol. 2. Springer; 2020. Chapter 25, Investigations on improving the efficiency of solar air heater using extended surfaces; 261-272.

[8] A.E. Kabeel, M.H. Hamed, Z.M. Omara, A.W. Kandeal. Influence of fin height on the performance of a glazed and bladed entrance single-pass solar air heater. Solar Energy. 2018; Vol. 162: 410-419.

[9] Kumar R., Chand P. Performance prediction of extended surface absorber solar air collector with twisted tape inserts. Solar Energy. 2018;Vol.169:40-8..

[10] Saravanan A, Jaisankar S. Heat transfer augmentation techniques in forced flow V-trough solar collector equipped with V-cut and square cut twisted tape. International Journal of Thermal Sciences. 2019 ;Vol.140:59-70.

[11] Vengadesan E., Senthil R. Experimental study on the thermal performance of a flat plate solar water collector with a bifunctional flow insert. Sustainable Energy Technologies and Assessments. 2022; Vol.50:101829.

[12] Reddy J., Das B., Negi S. Energy, exergy, and environmental (3E) analyses of reverse and cross-corrugated trapezoidal solar air collectors: An experimental study. Journal of Building Engineering. 2021 ;Vol.41:102434.

[13] A.D. Tuncer, A. Khanlari, A. Sozen, E.Y. Gürbüz, C. Sirin, A. Gungor. Energy-exergy and enviro-economic survey of solar air heaters with various air channel modifications. Renew. Energy. 2020; Vol. 160: 67-85.

[14] Kabeel A.E., Hamed M.H., Omara Z.M., Kandel A.W. On the performance of a baffled glazed-bladed entrance solar air heater. Applied Thermal Engineering. 2018;Vol.139:367-75.

[15] Debnath S., Das B., Randive P. Energy and exergy analysis of plain and corrugated solar air collector: Effect of seasonal variation. International Journal of Ambient Energy. 2020; 1-12.

[16] Jha P., Gupta R., Das B. Energy Metrics Assessment of a Photovoltaic Thermal Air Collector (PVTAC): A Comparison between Flat and Wavy Collector. EnergySources, Part A: Recovery, Utilization, and Environmental Effects. 2020; 1-19.

[17] H.J. Jouybari, S. Saedodin, A. Zamzamian, M.E. Nimvari, S. Wongwises. Effects of porous material and nanoparticles on the thermal performance of a flat plate solar collector: an experimental study. Renewable Energy. 2017; Vol 114: 1407–1418.

[18] Hussien S.Q., Farhan A.A. The effect of metal foam fins on the thermohydraulic performance of a solar air heater. Int. J. Renew. Energy Resour. 2019; Vol. 9: 840-847.

[19] Das B., Mondol JD., Debnath S., PugsleyA., Smyth M., Zacharopoulos A. Effect of the absorber surface roughness on the performance of a solar air collector: an experimental investigation. Renewable Energy. 2020; Vol 152: 567-572.

[20] Farhan A.A., M.Ali A.I, Ahmed H.E. Energetic and exergetic efficiency analysis of a v-corrugated solar air heater integrated with twisted tape inserts. Renewable Energy. 2021; Vol. 169: 1373-1385.

[21] Balaji K, Iniyan S., Swami M.V. Exergy, economic and environmental analysis of forced circulation flat plate solar collector using heat transfer enhancer in riser tube. Journal of Cleaner Production. 2017; Vol. 171: 1118-1127.

[22] Jafarkazemi F., Ahmadifard E. Energetic and exergetic evaluation of flat plate solar collectors. Renewable Energy. 2013; Vol. 56: 55-63.
[23] Gunjo D.G., Mahanta P., Robi P.S. CFD and experimental investigation of flat plate solar water heating system under steady state condition. Renewable Energy. 2017; Vol. 106: 24-36.
[24] Akram, N., Montazer, E., Kazi, S.N., Soudagar, M.E.M., Ahmed, W., Zubir, M.N.M., Afzal, A., Muhammad, M.R., Ali, H.M., Márquez, F.P.G., Sarsam, W.S. Experimental investigations of the performance of a flat-plate solar collector using carbon and metal oxides based nanofluids. Energy. 2021; Vol. 227:120452.
[25] Farahat, S., Sarhaddi, F., Ajam, H. Exergetic optimization of flat plate solar collectors. Renewable Energy. 2009; Vol. 34: 1169–1174.
[26] Luminosu I, Fara L. Determination of the optimal operation mode of a flat solar collector by exergetic analysis and numerical simulation. Energy. 2005; Vol. 30: 731–747
[27] Tong Y., Lee H., Kang W., Cho H. Energy and exergy comparison of a flat-plate solar collector using water, Al_2O_3 nanofluid, and CuO nanofluid. Journal of Applied Thermal Engineering. 2019; Vol 159: 113959.
[28] Rostami S., Sepehrirad M., Dezfulizadeh A., Hussein A.K., Goldanlou A.S., Shadloo M.S. Exergy Optimization of a Solar Collector in Flat Plate Shape Equipped with Elliptical Pipes Filled with Turbulent Nanofluid Flow: A Study for Thermal Management. Water. 2020; Vol. 12(8): 2294
[29] D.G. Gunjo, P. Mahanta, P.S. Robi, Exergy and energy analysis of a novel type solar collector under steady state condition: experimental and CFD analysis. Renewable Energy. 2017; Vol. 114: 655–669.
[30] Sakhrieh, A., Al-Ghandoor, A. Experimental investigation of the performance of five types of solar collectors. Energy Conversion and Management. 2013; Vol. 65: 715–720.
[31] Hashim WM, Shomran AT, Jurmut HA, Gaaz TS, Kadhum AA, Al-Amiery AA. Case study on solar water heating for flat plate collector. Case studies in thermal engineering. 2018;Vol.12:666-71.
[32] Alwan, N.T., Shcheklein, S.E. and Ali, O.M. Experimental analysis of thermal performance for flat plate solar water collector in the climate conditions of Yekaterinburg, Russia. Materials Today: Proceedings.2021; Vol. 42:2076-2083.